Evaluation of remaining fatigue life of concrete sleeper based on field loading conditions

You, Ruilin; Kaewunruen, Sakdirat

DOI:
10.1016/j.engfailanal.2019.06.086

Document Version
Peer reviewed version

Citation for published version (Harvard):
You, R & Kaewunruen, S 2019, 'Evaluation of remaining fatigue life of concrete sleeper based on field loading conditions', *Engineering Failure Analysis*, vol. 105, pp. 70-86. https://doi.org/10.1016/j.engfailanal.2019.06.086

Evaluation of remaining fatigue life of concrete sleeper based on field loading conditions

Ruilin You [a,b*], Sakdirat Kaewunruen [b]

[a]Railway Engineering Institute, China Academy of Railway Sciences, Beijing 100081, China

[b]School of Engineering, the University of Birmingham, Birmingham B15 2TT UK

*****Correspondence: s.kaewunruen@bham.ac.uk; Tel.: +44 (0) 1214 142 670

Abstract: The main functions of the sleepers in ballasted track include transferring loads and maintaining railway geometry. Sleepers can be manufactured using timber, concrete, steel or other engineered materials, but concrete is most used commonly around the world. There is much research on the impact load characteristics and the ultimate load carrying capacity of prestressed concrete sleepers, but research on the fatigue life of prestressed concrete sleepers is limited. A prestressed concrete sleeper's fatigue damage is mainly due to the repeated load of wheel-rail interaction. Fatigue failure is a time-dependent limited state where a concrete sleeper accumulates damage to a failure point. Concrete sleepers suffer fatigue loading throughout their whole lives, and the load-carrying capacity of concrete sleepers degrades as well. Therefore, fatigue life assessment is an important and complicated research topic. Field loading conditions, material time-dependent and dynamic properties, and the bending moments of prestressed concrete sleepers are analysed in this paper. This study also presents a fatigue life assessment method for concrete sleepers, and provides a study case based on field loading conditions and the time-dependent behaviour of material. This paper will improve concrete sleeper maintenance and inspection criteria, and will also provide the flexibility of a design principle for the concrete sleeper.

Keywords: Railway track; concrete sleeper; fatigue loads; remaining fatigue life; time-dependent; damage accumulation method.

1. Introduction

Railway sleepers are one of the most significant railway components that lie between the rail and the ballast [1].The functions of a sleeper include transferring and distributing the wheel-loads from the rail to the ballast bed, and maintaining the geometry of the railway track within a suitable range [2]. Concrete is the most common material for manufacturing railway sleepers around the world aside from North America where timber sleepers are more popular than concrete sleepers [3].At present, in many countries, the permissible stress (or allowable stress) method is adopted to design concrete sleepers [4, 5]. The permissible stress method does not accurately take into account the dynamic load, and underestimates the strength of the materials. Therefore, researchers have shown an increased interest in the limit states design method for concrete sleepers [2, 6-8]. Furthermore, many researchers have analyzed the damaged status of concrete sleepers.

Wakui. H and Okuda. H found that in Japan there were many unsolved problems in concrete sleepers which used a conventional design based on the permissible stress method[7]. For example, in some good quality lines the concrete sleepers are likely to be over designed, however, in some severe loading environment lines the concrete sleepers cracks develop rapidly due to the repeated impact loads. They put forward that a Fatigue Limit State (FLS) should be included in the process of a concrete sleeper design.

In order to clearly understand the reserved strength of concrete sleepers and to make a more economical design method of concrete sleepers, Leong. J used the field measurements and DTRACK simulations to establish the fatigue loading of the concrete sleepers and conducted some research into developing a limit state design methodology for concrete sleepers[9].

Kaewunruen, S. and Remennikov, A.M conducted experimental and numerical investigations about the dynamic behaviour of prestressed concrete sleepers subjected to impact loading. Among their research works, the fatigue impact damage and crack propagation in concrete sleepers were identified[10-13].

The limit state is a condition of a structure beyond which it no longer fulfils the relevant design criteria. Two limit states are commonly considered at the design stage of a reinforced and prestressed concrete structure: the Ultimate Limit State (ULS) and Serviceability Limit State (SLS) [14]. From the previous research, in addition to ULS and SLS, the limit states of concrete sleepers still include the FLS [7]. FLS is a time-dependent limit state where a concrete sleeper accumulates damage due to fatigue to a point where it is considered to have reached failure [11, 15]. For concrete sleepers, the FLS can still be divided into two different types according to the judgement criteria, the first one takes the cracking states as criteria (crack width or depth etc.), and the second one uses the fracture as criteria (reinforcement or prestressing steel fracture). From another view, the FLS includes the ULS and the SLS under fatigue loading. The latter will be researched in this paper.

Since concrete sleepers suffer fatigue loading throughout their lifespans and the load-carrying capacity of concrete sleepers degrades as well, the fatigue life assessment is an important and complicated research topic. Previous studies of concrete sleepers have not explored fatigue behavior in much detail. In this paper, the focus is on the fatigue life of a concrete sleeper calculation and the particular assessment method is based on the field loading condition and the time-dependent behaviour of material.

2. Fatigue life and assessment method

2.1. Structural performance over Life-Cycle

The fatigue failure of a member or a structure is considered to be the process of accumulated damage due to repeated loads over a long period of time. Therefore, the fatigue life of concrete sleepers can be determined by the service time to support the repeated train loads [11].

During the service life of the concrete sleeper, the train load will cause stress and deformation of the concrete sleeper, which will lead to the failure and damage of the concrete sleeper. The

deterioration state of the concrete sleeper is accelerating with the accumulation of operation time. The rate of deterioration of the concrete sleeper damage is related to the magnitude of the stress generated by the train load on the one hand (by the axle weight of the train, the running speed and the irregularity of the railway track, etc.) Impact), on the other hand, is also related to the self-generated resistance of the sleeper. The fatigue life of concrete sleepers is mainly controlled by the magnitude of stress generated from repeated loads and its own resistance. Since the loads generated from wheel-rail interaction are random, the fatigue damage of concrete sleepers are random affairs. In addition, the service life of a concrete sleeper is usually designed as 50 years [16], the fatigue loads generated from trains always increase because of the development of the economy, but the resistance of sleepers always decrease due to aging and deterioration. Considering these reasons, the life-cycle performance of a concrete sleeper can be considered as shown in Fig.1, in which uncertainties are associated with an initial performance indicator, deterioration rate, fatigue loads and maintenance/ repairs etc.

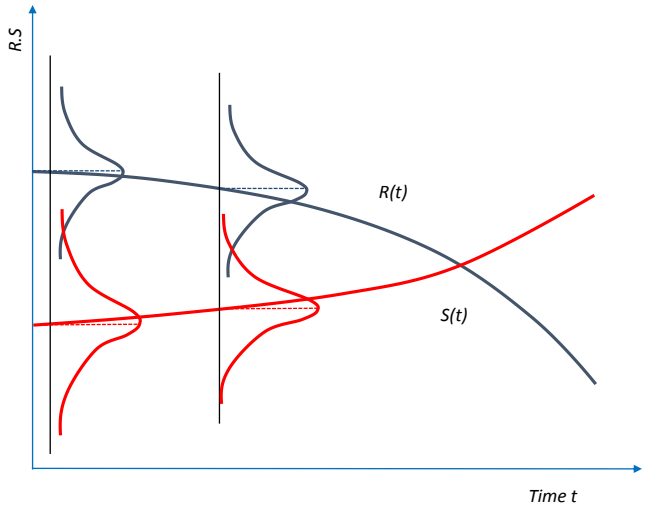

Fig. 1 Life-cycle performance of concrete sleeper

In Fig.1, R(t) is the probability distribution function of resistance, and S(t) is the probability distribution function of the load's effect. In general, the measure of risk associated with the specific event of R(t)<S(t) can be considered as the probability of the failure of the concrete sleepers. As

shown in Fig 1. , this interaction increases over the time causing a growth of the probability of failure. Structural models and their idealization, deterioration mechanisms, material resistances, geometries, and loads are uncertain. Therefore, a probabilistic approach has been researched to quantify the reliability of concrete sleepers [17].

Both the formulation and the detail process of this theory are beyond the scope of this paper. This study will focus on the fatigue life of concrete life based on the field loading condition. The time-dependent properties of the material and the damage accumulation process will also be considered.

2.2. The fatigue life assessment method

The Damage Accumulation Method which extended from the Miner's rule, has been used commonly in many design codes [18, 19].

For multiple cycles with variable amplitudes, the damage will be added based on the Damage Accumulation Method, and the cumulative damage index ($\sum$Di) is given by

$$\sum \mathrm{Di} = \sum_i \frac{n(\Delta\sigma_i)}{N(\Delta\sigma_i)} \qquad (1)$$

Where $n(\Delta\sigma_i)$ is the applied number of cycles for a stress range $\Delta\sigma_i$

$N(\Delta\sigma_i)$ is the resisting number of cycles for a stress range $\Delta\sigma_i$

This method has been used to evaluate the fatigue life of concrete life under constant amplitude cycled loads. During the experiment, the sleepers were supported as simply supported beams, and the applied loads were constant amplitude cycled loads, the results show a good agreement with the experiment results [20]. This method is defined in the CEB-fip model code [21] and EN 1992-2 [22], the maximum applied number of cycles for a single stress amplitude can be determined using the corresponding S-N curves (shown in Fig. 2). The S-N curve (also called "the stress-life curve") is the relationship between the stress level applied during fatigue and the number of cycles (life) when the structure is broken. S represents the stress level, which may be the maximum stress or the stress amplitude during the cycle. N represents the lifetime, which can be linear or logarithmic.

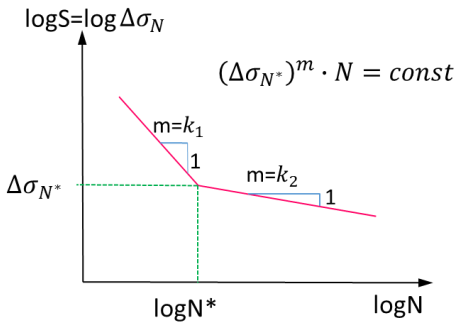

Fig. 2 S-N curves for steel[21] [22]

From Fig. 2, the failure cycle of the prestressing steel under a constant amplitude cyclic loading can be estimated by Eqs. 2 and 3:

If $(\Delta\sigma > \Delta\sigma_{N^*})$

$$logN_f = logN^* - k_1[\log(\Delta\sigma) - \log(\Delta\sigma_{N^*})] \quad (2)$$

If $(\Delta\sigma \leq \Delta\sigma_{N^*})$

$$logN_f = logN^* + k_2[\log(\Delta\sigma_{N^*}) - \log(\Delta\sigma)] \quad (3)$$

Where $\Delta\sigma$ is the stress range in the prestressed steel, $\Delta\sigma_{N^*}$ is the stress range at N* cycles which is given in Table 1.

Since the fatigue test data has a significant scatter and is influenced by the size of the sample and loading frequency etc., the curve in the CEB fib Model Code is expected to be a safe assumption. The parameters are, a lower bound to test the data and are appropriately conservative [23]. Loo et al. [23] suggested that the mean value of $\Delta\sigma_{N^*}$ for reinforced steel is 290 MPa, and Parvez and Foster [24] suggested the mean value of $\Delta\sigma_{N^*}$ is 300 MPa for the prestressing steel. In this paper, take the $\Delta\sigma_{N^*}$ as 300 MPa.

Table 1: Parameters of S-N curves for prestressing steel [21] [22]

S-N curve of prestressing steel used for	N*	Stress exponent k_1	Stress exponent k_2	$\Delta\sigma_{N^*}(MPa)$ at N* cycles
Pre-tensioning	10^6	5	9	185

$\Delta\sigma_{N^*}$ is the stress range obtained from a characteristic fatigue strength function.

Based on the fatigue loading conditions and the rules mentioned above, the fatigue life of a concrete sleeper can be calculated. The flow chart (see Fig. 3) presents the sequence for the fatigue analysis of a prestressed concrete sleeper. Fig.3 illustrates the fatigue life analysis based on the fatigue loads and the material properties' calculations. The value of the fatigue loads are variable. The loads will cumulate during the service life of a concrete sleeper. Meanwhile, the material (concrete and prestressed steel) properties are time-variant and will be influenced by dynamic loads as well[25-27].

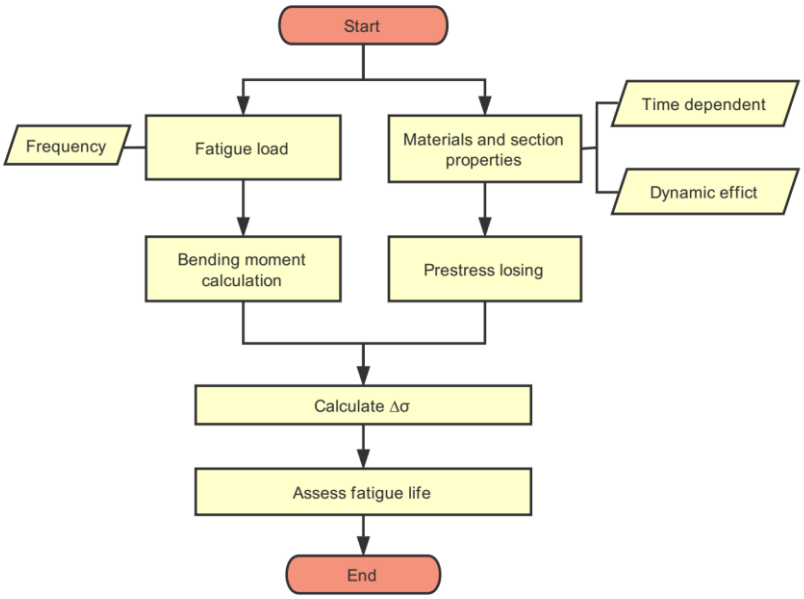

Fig. 3: Fatigue life assessment flow chart for concrete sleepers

2.3. Wheel-rail interaction fatigue load

The fatigue load research is the first important work to assess the fatigue life of concrete sleepers. Concrete sleepers are a significant component of railway tracks. One of its most important functions is to transfer the load from the rail to the ballast, so the fatigue load of concrete sleepers originates from the wheel-rail interaction. The wheel-rail interaction force is influenced by the train speed, traffic load, traffic density, curve radius of the rail line, the track quality and the environment etc.

146 The wheel-rail interaction force is different in different railways. Even in the same rail line, the force
147 will be changed with the time and the test section. Therefore, it is difficult to ascertain the precise
148 fatigue load of a concrete sleeper for its whole life. Therefore, static data (from test standard)
149 couldn't be used to predict the life of sleepers, and field data is much better to be used to accurately
150 predict the life of concrete sleeper. The good news is that there are some researchers who use the
151 wheel dynamic load detector to obtain the wheel-rail interaction force in the railway for a period (not
152 less than one year)[17], the data collected from the site test can be used to analyze and predict the
153 fatigue load for the railway track in the future.

154 In 2004, the Queensland University of Technology in Australia tested the impact force of two
155 separate sites, Braeside and Raglan. In these two sites, the maximum static axle load of operational
156 vehicles is 28 tons. The field measurement data in Braeside for full wagons was cited in the
157 following work (the data is shown in Tables 2 and Fig. 4)

158 Table 2: The impact wheel-rail interaction force from the site [9]

Impact force (kN)	Total wheels	Percentage	Cumulative frequency
＜50	1551481	96.383%	96.383%
50-60	4877	0.303%	96.685%
60-70	8302	0.516%	97.201%
70-80	13696	0.851%	98.052%
80-90	5426	0.337%	98.389%
90-100	10647	0.661%	99.051%
100-110	1956	0.122%	99.172%
110-120	3118	0.194%	99.366%
120-130	2877	0.179%	99.545%
130-140	2231	0.139%	99.683%

140-150	1701	0.106%	99.789%
150-160	1131	0.070%	99.859%
160-170	809	0.050%	99.909%
170-180	567	0.035%	99.945%
180-190	407	0.025%	99.970%
190-200	178	0.011%	99.981%
200-210	103	0.006%	99.987%
210-220	67	0.004%	99.991%
220-230	46	0.003%	99.994%
230-240	29	0.002%	99.996%
240-250	14	0.001%	99.997%
250-260	18	0.001%	99.998%
260-270	14	0.001%	99.999%
270-280	7	0.000%	99.999%
280-290	3	0.000%	100.000%
290-300	3	0.000%	100.000%
300-310	3	0.000%	100.000%
310-320	0	0.000%	100.000%
320-330	0	0.000%	100.000%
330-340	1	0.000%	100.000%
Sum	1609712	100%	

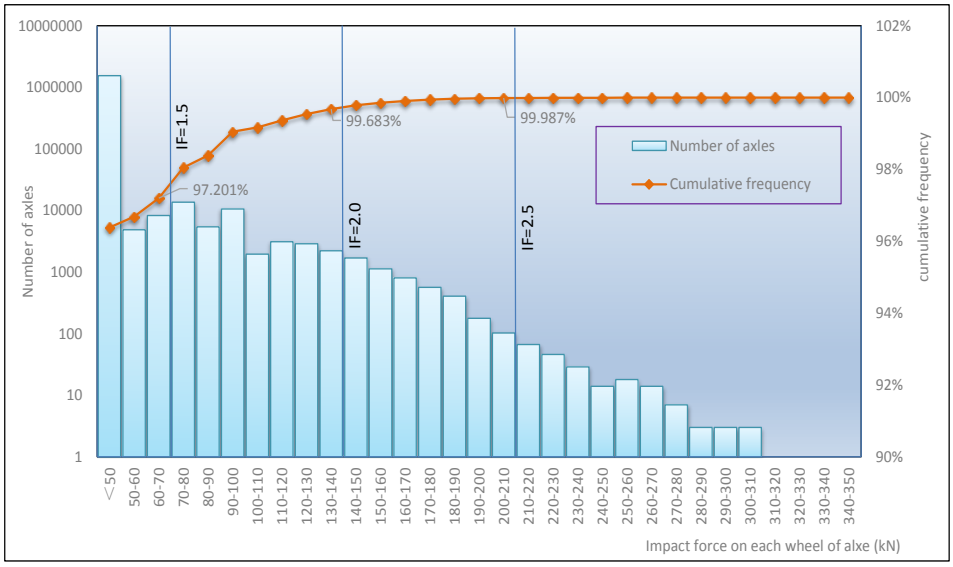

Impact Factor (IF) = 1+ (impact force) / (static wheel load)

Fig. 4: Typical impact force statistical data on the track at Braeside (2007) [9]

The field measurement data in Table 2 and Fig. 4 show that most of the impact forces are no more than 70kN, and the cumulative frequency of these data are 97.201%. This means that more than 97 percent of the dynamic loads' impact factors are less than 1.5. It can be found that there are a small number of impact loads greater than 210kN. The frequency of this extremely large impact force is less than 0.013%. These loads are probably caused by wheel flats, out-of round wheels, wheel corrugation, short and long wavelength rail corrugation, dipped welds and joints, pitting, and shelling etc.[12].

2.4. Bending moment of concrete sleepers

The bending moments of concrete sleepers are caused by the dynamic load on the railseat, and the railseat load are effected by the static wheel load, impact factor and distribution factor. According to AS 1085.14 [4], the railseat load R of a concrete sleeper can be calculated by the following equation

$$R=P\times DF\times IF \qquad (4)$$

Where

P is the static wheel load;

DF is the distribution factor.

The distribution factor DF is the distribution ratio of the wheel loads on a single sleeper, it's effected by the sleeper and axle spacing, track bed stiffness, fastener system elasticity and rail rigidity etc. For the sake of simplification, in the American Railway Engineering and Maintenance-of-Way Association (AREMA)[5]and the Australia Standard (AS)[4], the distribution factors are shown only as a function of sleeper spacing. According to AS 1085.14, the conservative estimation of the distribution is given in Fig. 5. In this paper, the spacing of a sleeper is taken as 600mm, and the distribution factor is 0.52 accordingly.

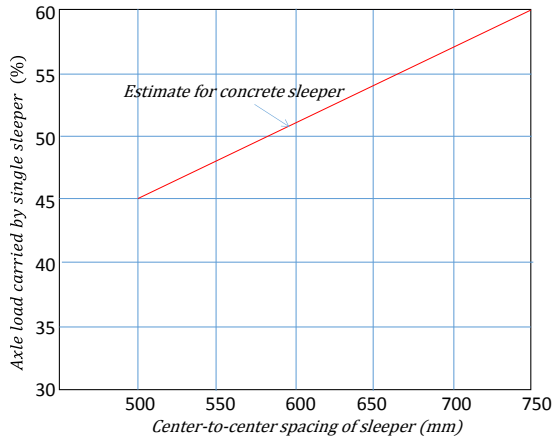

Fig. 5 Axle load distribution factor (DF)

Based on AS[4], the key sections' bending moments can be calculated using the following equations:

Maximum positive bending moment at railseat

$$\mathrm{M}_{RS+} = \frac{R}{8}(\mathrm{L} - \mathrm{g}) \qquad (5)$$

Maximum negative bending moment at railseat

$$\mathrm{M}_{RS-} = 0.67\mathrm{M}_{RS+} \qquad (6)$$

Maximum negative bending moment at centre

$$\mathrm{M}_{C-} = \frac{R}{4}(2\mathrm{g} - \mathrm{L}) \qquad (7)$$

Maximum positive bending moment at centre

$$M_{C+} = 0.05R(L - g) \quad (8)$$

Where

L is sleeper length (2.6m);

g is rail centre spacing (1.5m).

Using the impact force in Table 1 and Eqs.5~8, the bending moment at key sections of the concrete sleeper can be calculated, and the result is shown in Fig. 6. From Fig. 6, it can be seen that with the increasing of the impact force, the bending moments of the concrete sleeper are growing. The positive bending moment at railseat M_{RS+} is greater than the others, when the concrete sleeper suffers the same railseat load (R=210kN, the impact factor is 1.5), M_{RS+} is 14.8 kN.m, M_{RS-} is 9.9 kN.m, M_{C-} is 11.8 kN.m, and M_{C+} is 5.9 kN.m. When the impact factor increases to 2.5 (R=350kN), M_{RS+}, M_{RS-}, M_{C-} and M_{C+} will reach to 24.6kN.m, 16.5kN.m, 19.7kN.m, and 9.9kN.m separately. In addition, the frequency of the concrete sleeper's bending moments are the same as the impact force. These data will be used to assess the fatigue life of a concrete sleeper in subsequent sections.

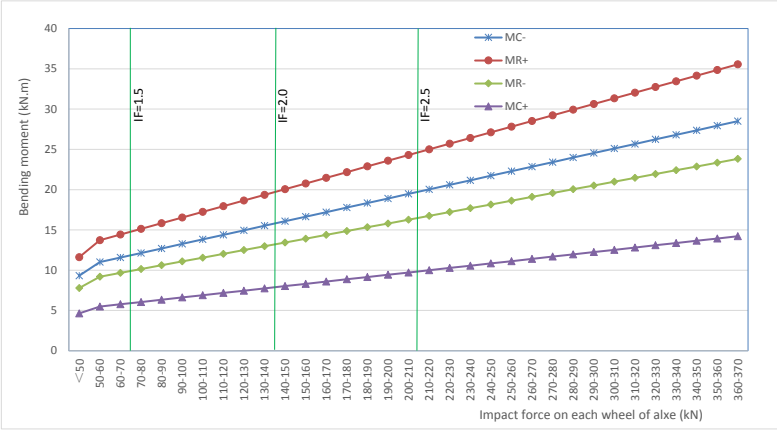

Fig. 6: bending moments of concrete sleeper developing with the impact force

3. Section and material properties

3.1. Section properties

In order to show the method to assess the fatigue life of one kind of concrete sleeper which used in Australian railway was studied as an example. Material and section properties of the assessed concrete sleeper are referenced to [24, 28], and a few modifications and supplements are made. In the study case, the concrete sleeper meets all the requirements of AS 1085.14[4] ,and consists of 18 prestressing wires with 26.4 kN prestressing force per wire. The geometry detail of the railseat and centre section can be seen in Fig. 7.

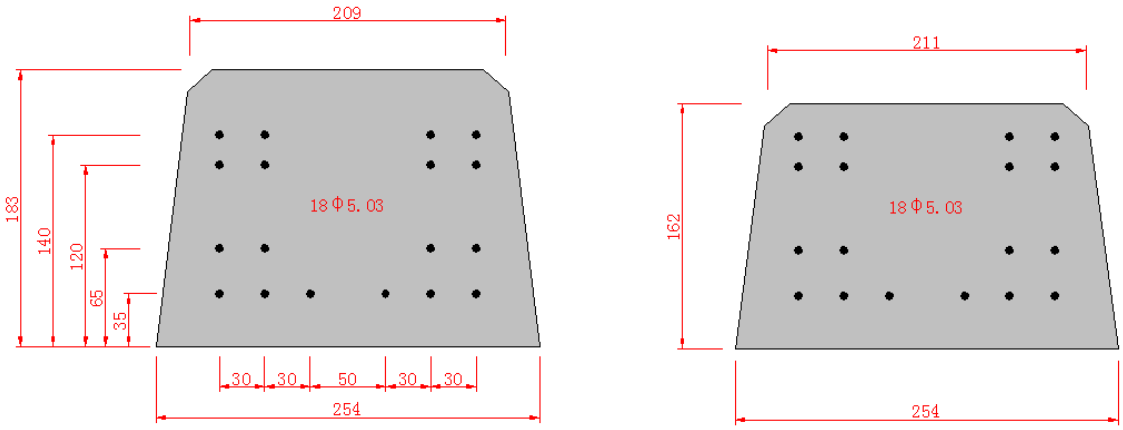

(a) Railseat section (In: mm) (b) Centre section (In: mm)

Fig. 7: Railseat and centre sections of sleeper (mm) [24, 28]

Based on the geometry of the concrete sleeper, the other important parameters of the section are calculated and shown in Table 3.

Table 3 Section parameters of railseat and centre sections

Parameters	Railseat section	Centre section
Area of single prestressing wire A_{ps} (mm^2)		19.6
Total area of prestressing wires A_p(mm^2)		353.5
Initial prestress per wire σ_{si}(MPa)		1328.4
Modulus of elasticity ratio of prestressing wire and concrete n_e		5.56

Area of concrete section $A_c(\text{mm}^2)$	42141.2	37442.0
Distance from the centre of gravity of the concrete from the soffit $y_c(\text{mm})$	88.1	78.0
Distance from the centre of gravity of the prestressing wires from the soffit y_p (mm)	83.9	83.9
Transformed area $A_t(\text{mm}^2)$	43751.5	39052.2
First moment about the bottom fibre $S_t(\text{mm}^3)$	3846038.3	3057054.4
Distance of the centroidal axis of transformed area from the soffit $y_{\text{t}}(\text{mm})$	87.9	78.3
Eccentricity of the centroid of prestressing force $e(\text{mm})$	-4.0	5.6
Moment of inertia of transformed section about its centroidal axis $I_t(\text{mm}^4)$	119085167.6	83806252.2

3.2. The concrete and prestressed steel's original properties

The properties of the concrete sleeper's material which have been calculated in this study are shown in Table 4. The impact and time-dependent behavior will be discussed in following section.

Table 4 Original materials properties

Materials' properties		symbol	Value
Concrete	Mean compressive strength	f_{cm}	85MPa
	Flexural tensile strength	f_{cf}	5.8MPa
	Modulus of elasticity	E_c	43.8GPa
Prestressed wire	Ultimate tensile strength	f_{pb}	1950MPa
	Yield strength	f_{py}	1620MPa
	Modulus of elasticity	E_s	200GPa

3.3. The strain rate effect's impact

During the impact loading, the materials' properties will be effected by the stress rate $\dot{\sigma}$ and strain rate $\dot{\varepsilon}$. The change in properties due to the impact effects is usually expressed as a relation between

231 the relative value of the property and logarithm of the strain rate. With the research presented by
232 Wakui and Okuda [7, 29, 30], the dynamic material properties of the concrete can be determined as
233 follows:

234 $$\frac{f_{cm,im}}{f_{cm}} = 1.49 + 0.268\log_{10}\dot{\varepsilon}_c + 0.035[\log_{10}\dot{\varepsilon}_c]^2 \quad (9)$$

235 Where

236 $f_{cm,im}$ is the dynamic compressive strength of concrete

237 $\dot{\varepsilon}_c$ is the strain rate of concrete

238 Based on the CEB-fip model code [21], for a given strain rate (less than 30 s^{-1}) the compressive
239 strength can be estimated from Eq. (10)

240 $$\frac{f_{cm,im}}{f_{cm}} = \left(\frac{\dot{\varepsilon}_c}{\dot{\varepsilon}_{c0}}\right)^{1.026\alpha_s} \quad (10)$$

241 Where

242 $\dot{\varepsilon}_{c0}$ =$30 \times 10^{-6}s^{-6}$

243 α_s is the coefficient calculated as follows

244 $$\alpha_s = \frac{1}{5+9f_{cm}/f_{cm0}} \quad (11)$$

245 Where

246 f_{cm0}=10MPa

247 The calculation results between the equation of CEB-fip model code and the equation used by
248 Wakui and Okuda were contrasted in Fig.8. Figure 8 illustrates that, when the strain rate less than
249 1.5×10^{-2}, the effect of the impact calculated by equation (9) is less than that calculated by equation
250 (10), but with the increasing strain rate, the former's results are bigger than the latter's. In this study,
251 the equation of the CEB-fip model code will be used in order to get a conservative result, and the
252 strain rate is approximately 2, based on the previous experiments and recommendations [7, 29, 30].

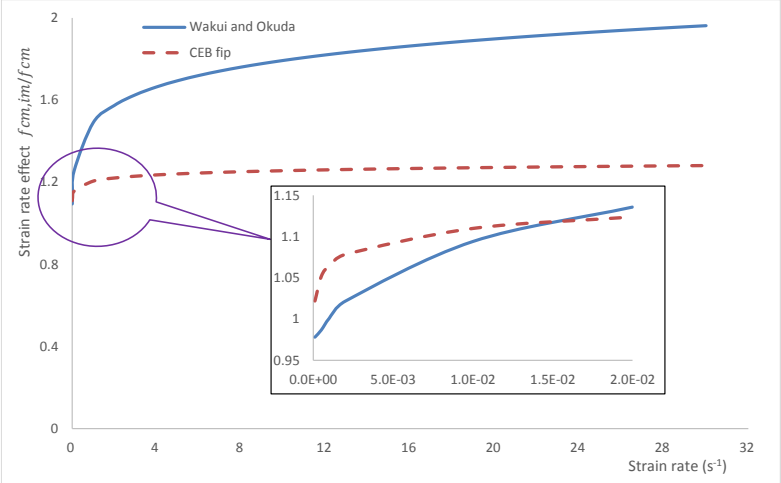

Fig. 8: Strain rate effect to the compressive strength of concrete

In the CEB-fip model code, the dynamic effects on the properties of prestressing steel are not given. Wakui and Okuda used the following equation to calculate the impact effect on the prestressing steel [7, 29, 30]

$$\frac{f_{\mathrm{py,im}}}{f_{\mathrm{py}}} = 10^{0.38 \log_{10} \dot{\varepsilon}_{py}{}^{-0.258}} + 0.993 \qquad (12)$$

Where

$f_{\mathrm{py,im}}$ is the dynamic yield strength of prestressing steel

$\dot{\varepsilon}_{py}$ is the strain rate of prestressing steel

Based on the previous experience[7], the average total duration of impact forces is about 4ms, and the dynamic ultimate strain of prestressing steel is about 20×10^{-3}.Since the impact stress wave will be delayed during the stress propagation, the total duration of the impact force influencing the reinforcement in the concrete sleeper is roughly about 6 ms [7, 29, 30]. It is then estimated that the strain rate in prestressing steel is approximately 6. According to Eqs. (10) ~ (12), the dynamic properties of materials can be obtained.

3.4. Degradation of the material properties-time-dependent

For concrete sleepers exposed to damaging environments, the life-cycle performance must be considered as time-dependent. Aside from the uncertainty in the initial material and geometrical

properties, the degradation process of the materials is effected by various factors, including chemical (acid, carbonate aggregate, silicate aggregate, chlorides and sulphates etc.), physical (temperature change, frost and abrasion etc.), mechanical (cyclic loading), and biological (micro-organisms) factors. Mechanisms of great complexity, in which several mechanisms play a part in and/or affect a mechanism in turn constitute a degradation factor [31]. It can be seen that the degradation of material properties is complicated. A measurement of the time-variant structure performance is realistically possible only in probabilistic terms. This work could not be carried out within the scope of this research. In this study, the strength degradation of concrete and prestressing steel will be simplified as follows in the experiential and experimental equations[32, 33].

$$f_{cm}(t) = f_{cm}(1 - 8 \times 10^{-7} t^3) \quad (13)$$

$$f_{py}(t) = f_{py}(1 - 2.2 \times 10^{-6} t^3) \quad (14)$$

Where

t is the age of concrete structures (in years).

Based on Eqs. (13), (14), the time-dependent curves of material properties in this study are shown in Fig.9.

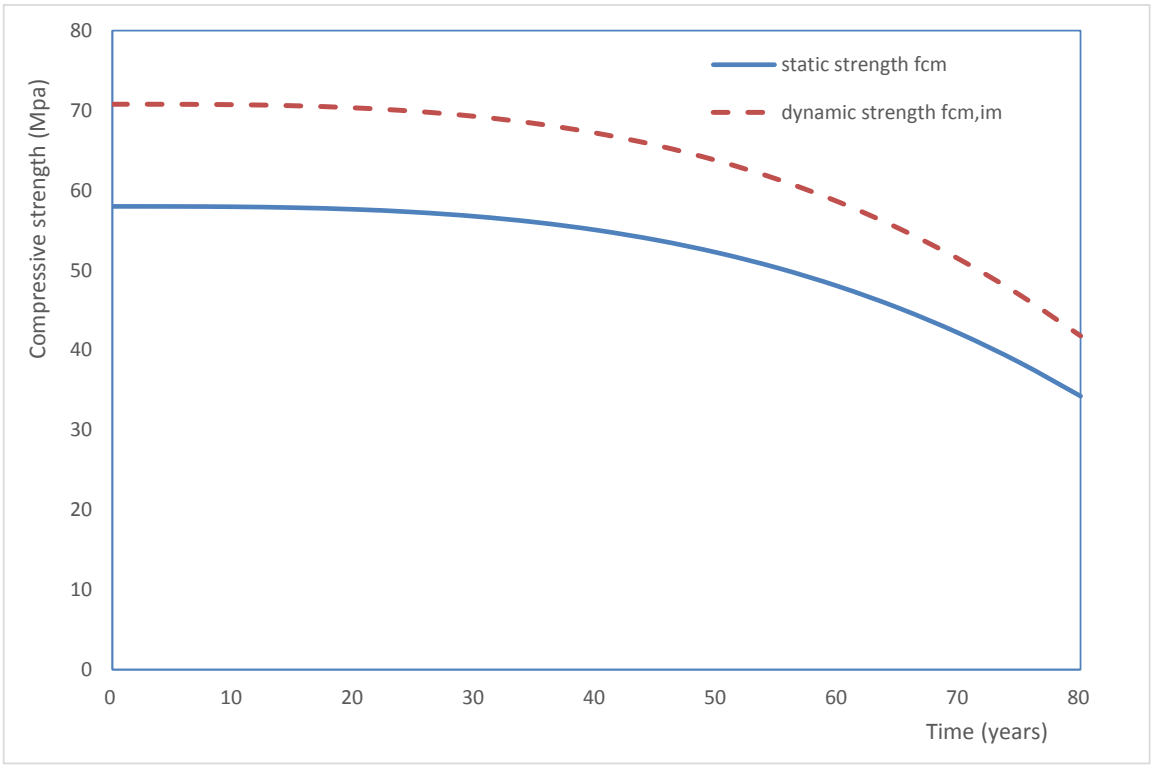

a) Concrete compressive strength

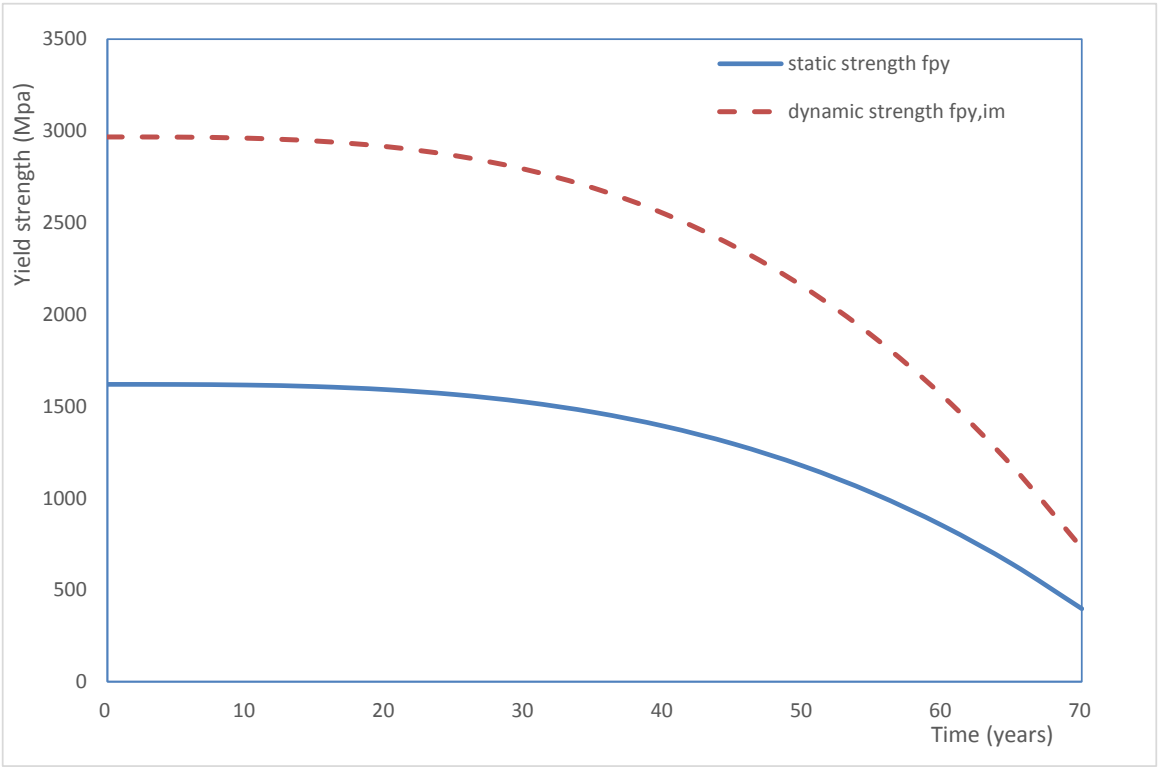

(b) Prestressing steel yield strength

Fig. 9 Time-dependent curve of material properties

Fig.9 illustrates that the material properties' degradation rate increases during the concrete structure's service life. At the earliest period of 30 years, the degradation speed of the material is slow, but after that, the speed increases sharply. It should be noted that, Eqs. (13), (14) were gained from the stick environment. These results are conservative for prestressed concrete sleepers and therefore, the fatigue life calculated from this study is conservative.

4. The calculation of prestress losses

Similarly to other prestressed concrete (PC) members, the prestress of concrete sleepers will be lost after being transformed [34-38]. The prestress loss consists of both instantaneous losses and time dependent losses. The instantaneous losses take place due to the elastic shortening of the concrete. The time-dependent losses are due to the creep and shrinkage of the concrete and the relaxation of tendons. Based on AS3006[34], the losses of prestress for the concrete sleeper in this study are given in Table 5. The time used as an example in the table is 2 years (730 days).

The loss of prestress due to shrinkage is greater than the others both in the railseat section and the centre section of the concrete sleeper, and the total loss percentage in these two key sections is around 24% in both.

Table 5: The prestress loss of the concrete sleeper

Loss due to	Railseat section		Centre section	
	Loss of prestress (MPa)	Percentage of initial prestress	Loss of prestress(MPa)	Percentage to initial prestress
Elastic shortening	74.1	5.5%	82.9	6.2%
Creep	81.0	6.0%	84.6	6.3%
Shrinkage	103.3	7.7%	95.7	7.1%
Tendon	59.1	4.4%	58.9	4.4%

relaxation				
Total	317.5	23.6%	322.0	24.0%

Since the loss due to creep, shrinkage and tendon relaxation are influenced by time, these time-dependent losses at the railseat and the centre sections of the concrete sleeper are calculated and shown in Fig.10. From these two figures, it can be found that at the early age of the concrete sleeper, the losses are increased rapidly, then after 2 years (730 days), the trend decreases.

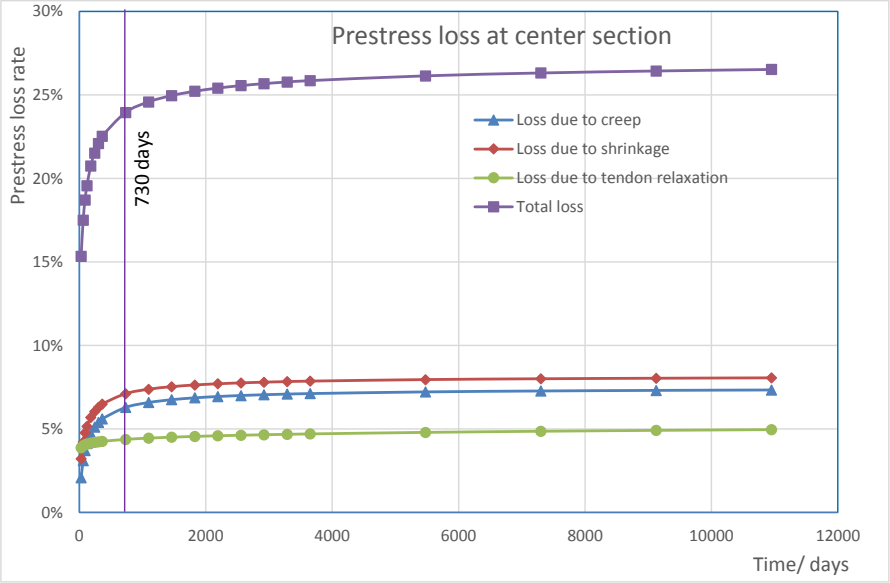

(a) Railseat section

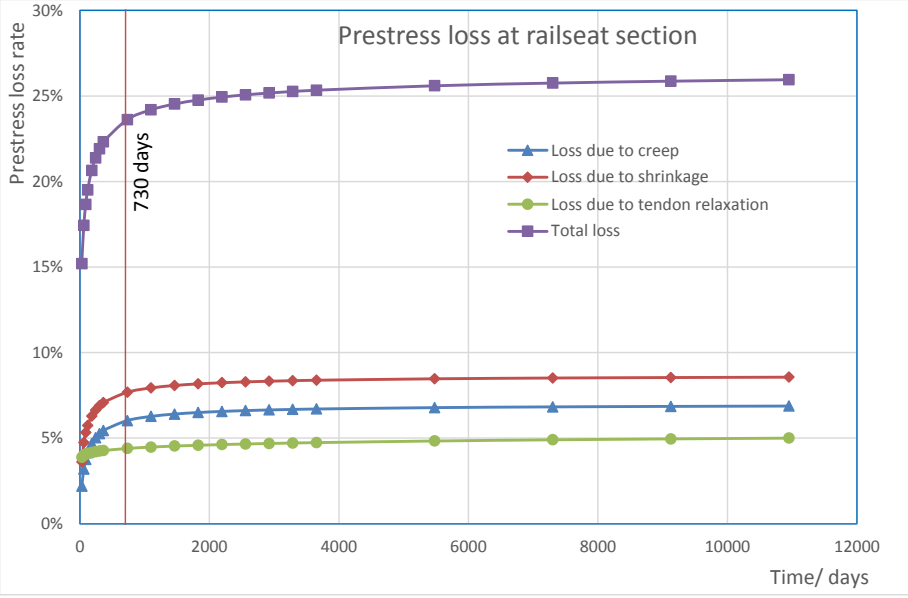

(b) Centre section

Fig. 10 Time-dependent loss of concrete sleeper developing over time

5. Fatigue life assessment

5.1. Cracking load calculation

The status of a concrete sleeper during loading, can be divided into two stages. In the first stage, no cracking appeared. Linear relations are assumed between stress and strain for both concrete and steel, and strains at different levels in the sleeper are assumed to vary linearly with depth. Based on the material and section properties mentioned above, the concrete stress at the bottom fiber due to the prestress force is:

$$\sigma_{cF}^{b} = \frac{nA_{ps}\sigma_{\mathrm{se}}}{A_t} + \frac{nA_{ps}\sigma_{\mathrm{se}}e}{I_t} y_{\mathrm{t}} \qquad (15)$$

Here, σ_{se} is the effective prestress per wire after losss.

The cracking moment M_{cr} is

$$M_{\mathrm{cr}} = I_t \cdot \frac{\sigma_{cF}^{b} + f_{cf}}{y_{\mathrm{t}}} \qquad (16)$$

Taking the prestress after 2 years (730 days) as an example, the cracking moment and the decompression moment (when prestressing stress was overcome) of the concrete sleeper were calculated. The results are provided in Table 6.

Table 6: The cracking moment and the decompression moment of a concrete sleeper (kN.m)

Location	Decompression moment	Cracking moment
The positive direction at the railseat section	12.7	18.7
The negative direction at the railseat section	8.9	14.5
The negative direction at the centre section	11.3	15.7
The positive direction at the centre section	7.9	12.6

Using the relationships between loads and bending moments, the impact loads which generated the cracking and the decompression could be calculated. Based on the field test results given in the

334 above section, the impact loads that cause the cracking moment and the decompression moment at

335 the railseat section and the centre section are shown in Fig.11 and Fig.12.

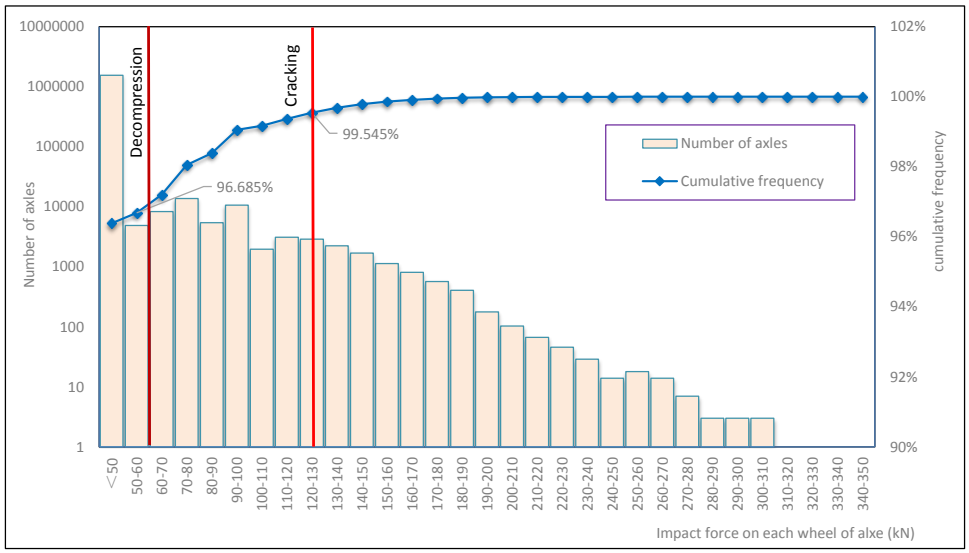

336

337 (a) Positive direction (M_{R+})

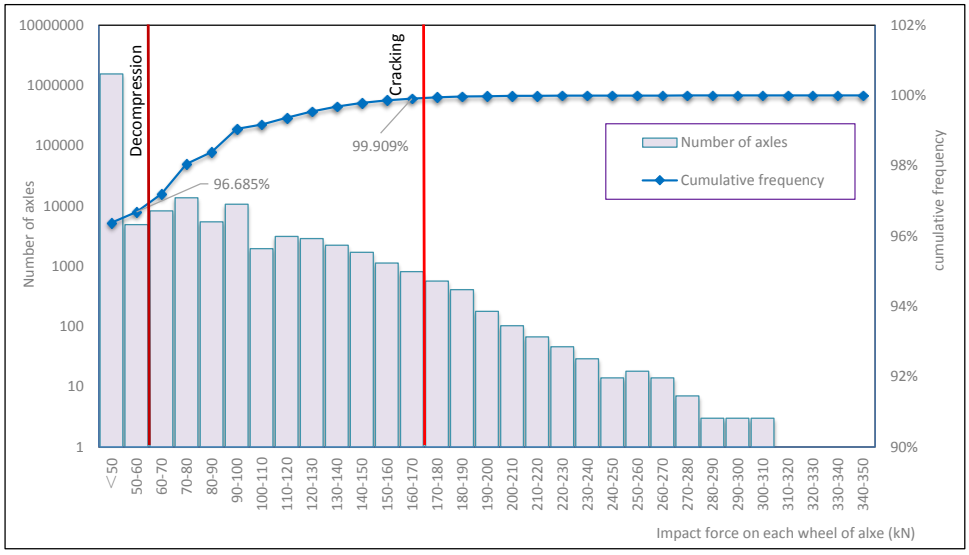

338

339 (b) Negative direction (M_{R-})

340 Fig.11 The impact loads which lead to the cracking moment and the decompression moment at the

341 railseat section

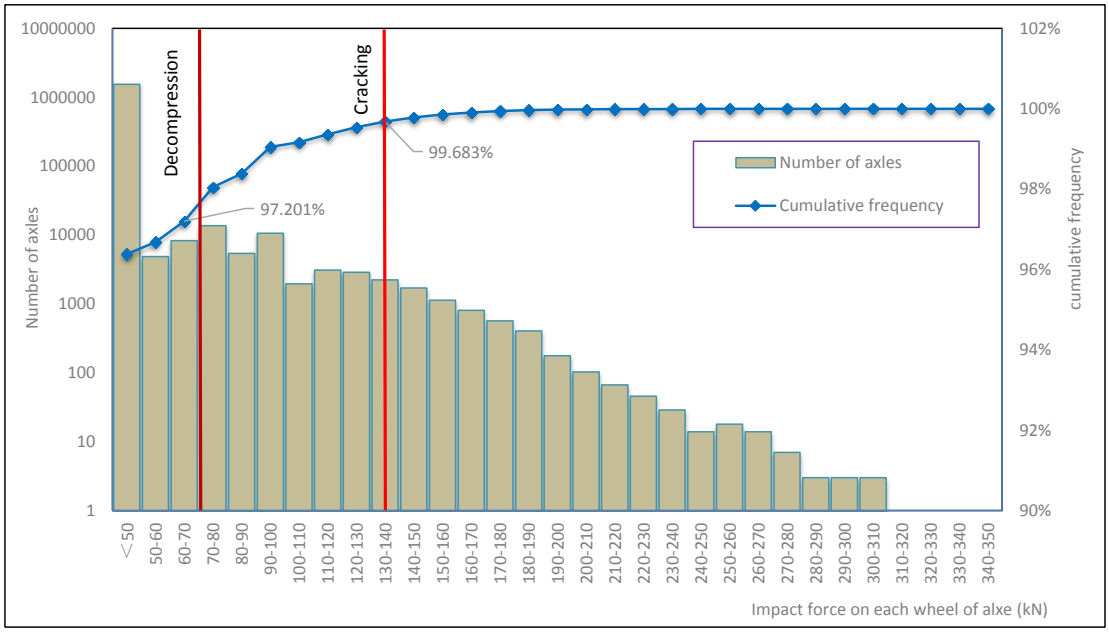

(a) Negative direction (M_{C-})

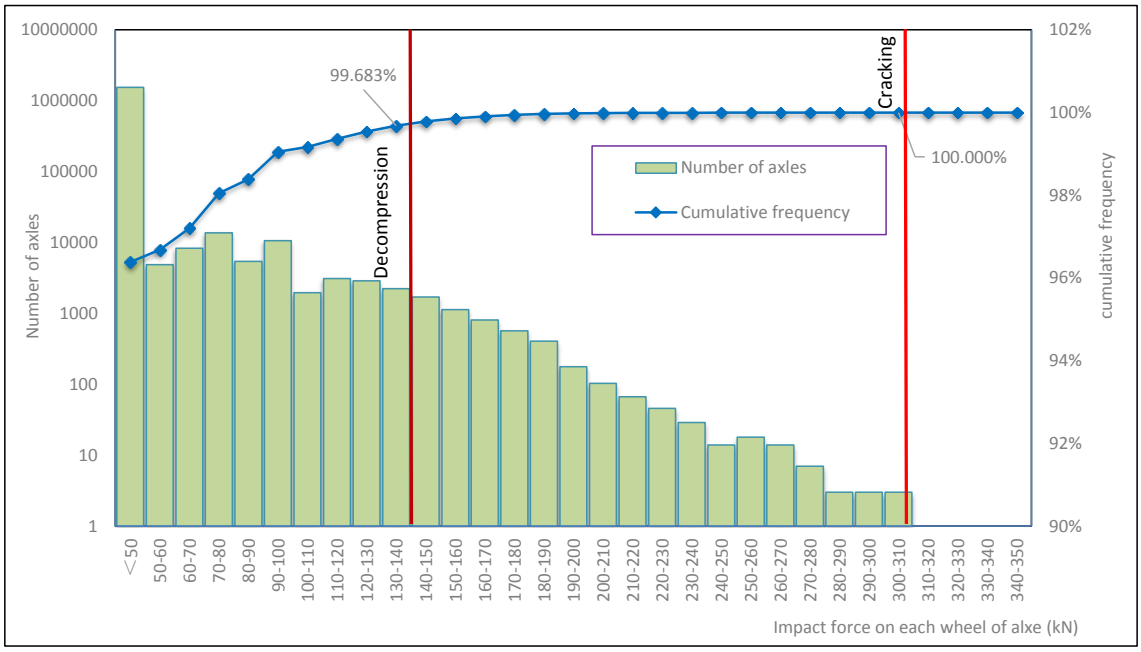

(b) Positive direction (M_{C+})

Fig.12 The impact loads that cause the cracking moment and the decompression moment at the centre section

From Fig.11, it can be found that more than 96.7% impact loads cannot generate the decompression bending moment at the railseat section; more than 99.5% impact loads cannot cause positive flexure cracking; and more than 99.9% impact loads cannot cause negative flexure cracking.

Fig.12 illustrates that, for the negative direction at the centre section of the concrete sleeper, more than 97.2% impact loads cannot generate the decompression bending moment, and more than 99.6% impact loads cannot cause negative flexure cracking. Since the positive bending moment at the centre section in the railway lines is smaller than the others, the impact loads that cause decompression and cracking are higher accordingly, almost 100% impact loads cannot cause positive flexure cracking.

From the other view, Fig.11 and Fig.12 show that there are still a few extreme impact loads that can generate the cracking moment at both the railseat section and the centre section. The frequency of such events is small. The fatigue life calculation in the subsection does not take the tensile strength of concrete into account.

5.2. Calculating the Remaining Fatigue Life

As the crack progresses, the status of the concrete sleeper arrives at the second stage. The neutral axis of the concrete section will change when the section is fully cracked. The prosperity of the section can be calculated.

The distance from the centre gravity of the effective transformed area to the top of the compressed area y_{CG} can be trialled as follow.

$$y_{CG} = \text{root}\Big[\big[S_{pcII} - n_e A'_{p4}(h - y_{cg} - d_4) - n_e A'_{p3}(h - y_{cg} - d_3) - n_e A'_{p2}(h - y_{cg} - d_2) - n_e A'_{p1}(h - y_{cg} - d_1)\big], y_{cg}\Big] \quad (17)$$

Where the S_{pcII} is the first moment about the bottom fibre after cracking, A'_{pi} is area of the prestressed steel in layer i, and d_i is the distance from the prestressed steel in layer i to the bottom of tension area.

Using the transformed area of concrete section A_{cII}, the effective transformed section can be calculated as:

$$A_{tII} = A_{cII} + n_e A_p \qquad (18)$$

The moment of inertia of the fully cracked section is:

$$I_{cr} = I_{ccr} + n_e A'_{p4}(h - y_{cg} - d_4)^2 + n_e A'_{p3}(h - y_{cg} - d_3)^2 + n_e A'_{p2}(h - y_{cg} - d_2)^2 + n_e A'_{p1}(h - y_{cg} - d_1)^2 \qquad (19)$$

The effective moment of inertia in the life time is:

$$I_{ef} = I_{cr} + (I_t - I_{cr})(\frac{M_{cr}}{M_{max}})^3 \qquad (20)$$

Where I_t is the moment of inertia of the transformed section before cracking; M_{cr} is the cracking moment; and aM_{max} is the maximum bending moment at the section under the cyclical load.

Then, the tension stress range in the first layer of prestressed steel at the tension area is:

$$\Delta\sigma_{pt1} = n_e \frac{M_{max} - M_{min}}{I_{ef}}(h - y_{cg} - d_1) \qquad (21)$$

Where, M_{min} is the minimum bending moment at the section under the cyclical loads.

The concrete sleeper takes on the fatigue load throughout its whole life and each wheel that passes by can be seen as a cyclical load. In each loading cycle, the peak of the dynamic load can be taken as the maximum load and the minimum load is 0. For any dynamic load, the tension stress range of the concrete sleeper's prestressed steel can be calculated, and the failure load numbers of the concrete sleeper can be calculated based on the method presented in section 2. As mentioned before, the material properties and prestress loss value are developed with time and the damage index in each year is calculated in this study. Since the wheel-rail interaction fatigue loads are varied randomly, the percentage of each force range gathered from the field test (given in the previous section) were taken into account as well. Assuming the total number of wheels (1609712) passing on the concrete sleeper remain the same every year, the damage index of the key section of the concrete sleeper each year (Di) was reached, and is presented in Fig.13 (a). And then, the accumulated damage index ($\sum$Di) can

398 be calculated accordingly (shown in Fig.13 (b)).Since the tension stresses' range in the first layer of
399 prestress steel caused by the positive bending moment at the centre of the concrete sleeper is small,
400 the fatigue life can be seen as infinite. This is not illustrated in Fig.13.

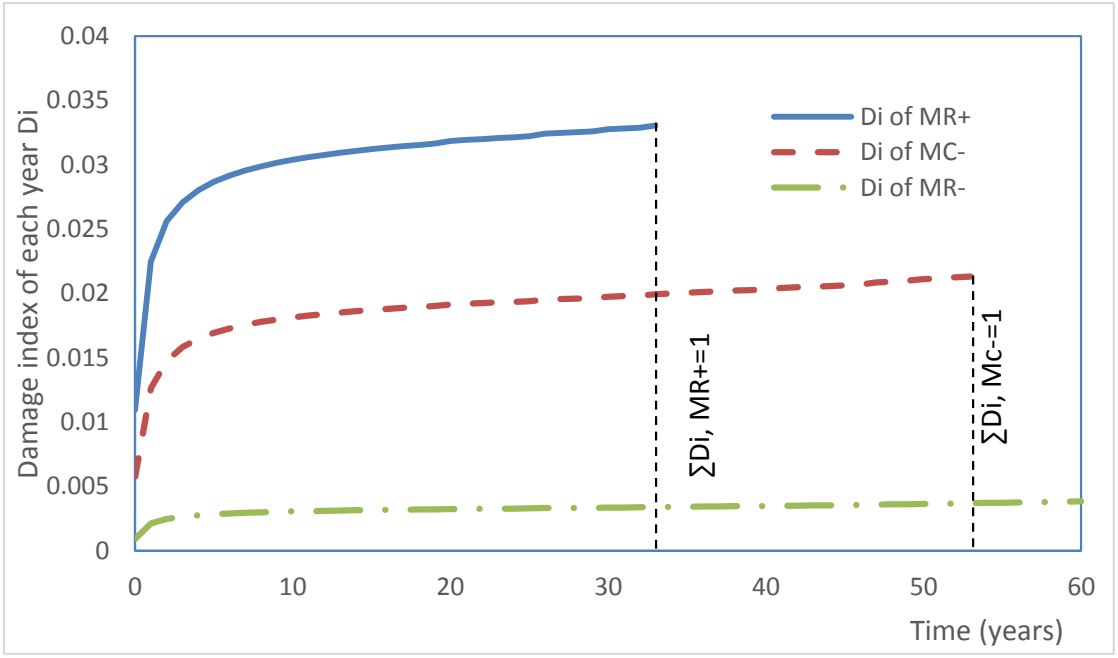

401

402 (a) Damage index of each year

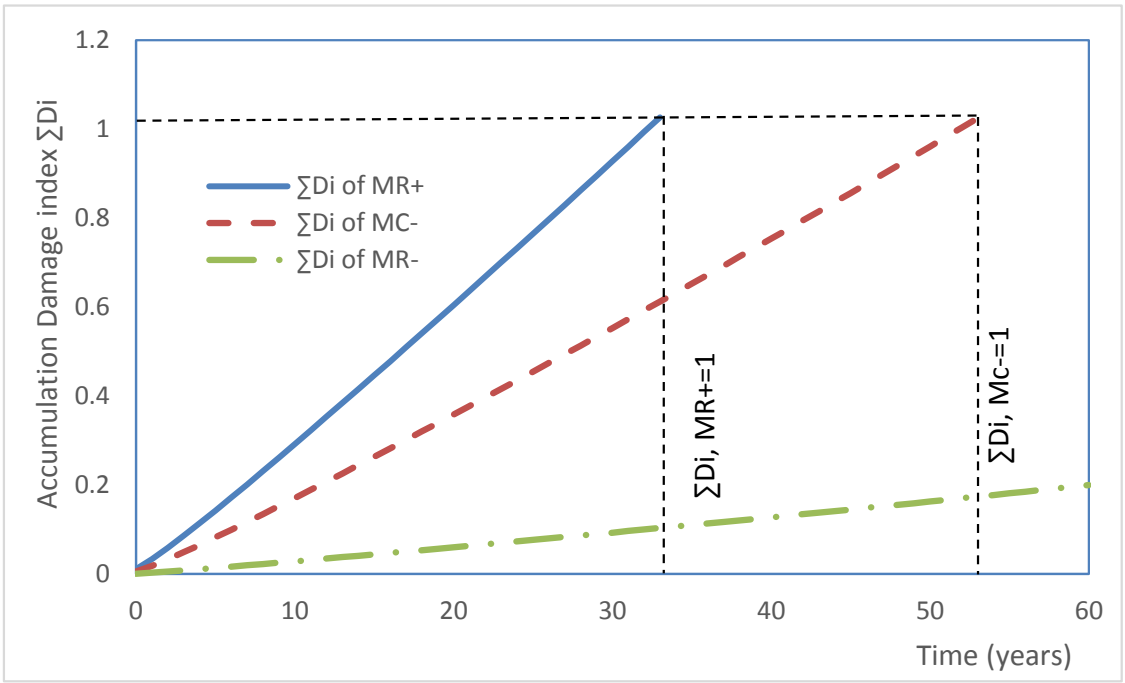

403

404 (b) Accumulated damage index

405 Fig. 13 Damage index of each year and the accumulated damage index developing with time

Fig.13 illustrates that at the early age of the concrete sleeper, because of prestress loss, the damage indexes of different sections increase sharply. Two years later, since the prestress loss and material properties remain steady, the damage indexes develop slowly. From Fig.13, it can be found that the accumulated damage index caused by positive bending moment at the railseat increases to 1 after 33 years. This means that the concrete sleeper's fatigue life of the railseat section is about 33 years. Due to the negative bending moment at the centre section, the fatigue life of a concrete sleeper is 53 years. Since the damage index calculated shows that the negative bending moment at the railseat section is small, the life based on the fatigue loads is much longer than 60 years. Therefore, the fatigue failure of the concrete sleeper at the railseat section is controlled by the positive bending moment, and the fatigue life is around 33 years. The fatigue failure of the concrete sleeper at the centre section is controlled by the negative bending moment, and the fatigue life is around 53 years.

6. Conclusions

In this paper, a method based on the damage accumulation concept to assess the fatigue life of a concrete sleeper is demonstrated. Fatigue load analysis and the materials' properties are two important elements to calculating the fatigue life of a concrete sleeper.

During the service life of a concrete sleeper, the material properties will be influenced by impact loading and degradation. The results show that up until 30 years the degradation speed of material is slow, but after that the speed increases sharply. The conserved equations were used in this study to reach the time-dependent material properties. Based on the concrete sleepers that served in the Australia railway, the instantaneous losses and time-dependent losses of prestress are both studied in this paper. Taking 2 years (730 days) as an example, the total prestress loss percentage in the railseat section and the centre section of a concrete sleeper are both around 24%, and the loss of prestress due to shrinkage is greater than the other influencing factors.

The results of the calculations regarding the cracking moment and the decompression moment of a concrete sleeper show that: more than 96.7% impact loads cannot generate the decompression bending moment at the railseat section; and more than 99.5% impact loads cannot cause positive flexure cracking. There are only a few extreme impact loads which can generate a cracking moment at the railseat section and the centre section. These events are rare.

After the fatigue loads and load bearing capability calculation, the fatigue life of concrete sleepers can be researched using the damage accumulation method. The results show that the fatigue failure of a concrete sleeper at the railseat section is controlled by the positive bending moment, and the fatigue life is around 33 years; the fatigue failure of a concrete sleeper at the centre section is controlled by the negative bending moment, and the fatigue life is around 53 years.

The fatigue life of concrete sleepers is affected by lots of factors, such as material properties, manufacturing quality, density of the train, and maintenance of the vehicle and/or railway etc. Evaluating the fatigue life is a complicated problem and needs more research to be done. In the study, a simplified method is shown. However, the outcomes of this paper will improve the concrete sleeper maintenance and inspection criteria and provide the flexibility of FLS design for concrete sleepers.

Acknowledgements

The first author wishes to thank the China Academy of Railway Sciences (CARS) for financial sponsorship of the collaborative project at the University of Birmingham (UoB). The first author also wishes to gratefully acknowledge the help from the Birmingham Centre for Railway Research and Education (BCRRE) at work in the UoB. All authors send special thanks to the European Commission for H2020-MSCA-RISE, Project No. 691135 “RISEN: Rail Infrastructure Systems Engineering Network” (www.risen2rail.eu) [39].

References

[1] J. Zhao, A.H.C. Chan, M.P.N. Burrow. Reliability analysis and maintenance decision for railway sleepers using track condition information. Journal of the Operational Research Society. 58 (2007) 1047-55.

[2] S. Kaewunruen. Experimental and numerical studies for evaluating dynamic behaviour of prestressed concrete sleepers subject to severe impact loading. Wollongong, Australia: University of Wollongong; 2007.

[3] W. Ferdous, A. Manalo. Failures of mainline railway sleepers and suggested remedies – Review of current practice. Engineering Failure Analysis. 44 (2014) 17-35.

[4] AS1085.14, Railway track material Part 14: Prestressed concrete sleepers, Standards Australia, Australia, 2003.

[5] AREMA, AREMA-Manual for Railway Engineering, Chapter 30 Ties, American Railway Engineering and Maintenance-of-Way Association, Maryland, American 2016.

[6] N. Wang. Resistance of concrete railroad ties to impact loading. Canada: University of British Columbia; 1996.

[7] H. Wakui, H. Okuda. A Study on Limit State Design Method for Prestressed Concrete Sleepers. Doboku Gakkai Ronbunshu. 1997 (1997) 35-54.

[8] R. Gustavson. Structural behaviour of concrete railway sleepers. Sweden: Chalmers University of Technology; 2002.

[9] J. Leong. Development of a limit state design methodology for railway track. Australia: Queensland University of Technology; 2007.

[10] S. Kaewunruen, A. Remennikov. Experimental and numerical studies of railway prestressed concrete sleepers under static and impact loads. Civil Computing. 3 (2007) 25-8.

[11] S. Kaewunruen, A.M. Remennikov, M.H. Murray. Introducing a new limit states design concept to railway concrete sleepers: an Australian experience. Frontiers in Materials. 1 (2014) 8.

[12] S. Kaewunruen, A. Remennikov. On the residual energy toughness of prestressed concrete sleepers in railway track structures subjected to repeated impact loads. Electronic Journal of Structural Engineering. 13 (2013) 41-61.

[13] A. Remennikov, M.H. Murray, S. Kaewunruen. Reliability-based conversion of a structural design code for railway prestressed concrete sleepers. Proceedings of the Institution of Mechanical Engineers, Part F: Journal of Rail and Rapid Transit. 226 (2012) 155-73.

[14] EN1990, Eurocode - Basis of structural design, European Committee for Standardisation, Brussels 2002.

[15] A.M. Remennikov, M.H. Murray, S. Kaewunruen. Reliability-based conversion of a structural design code for railway prestressed concrete sleepers. Proceedings of the Institution of Mechanical Engineers, Part F: Journal of Rail and Rapid Transit. 226 (2011) 155-73.

[16] S. Kaewunruen, R. You, M. Ishida. Composites for Timber-Replacement Bearers in Railway Switches and Crossings. Infrastructures. 2 (2017) 13.

[17] S. Kaewunruen, A. Remennikov, M.H. Murray. Limit states design of railway concrete sleepers. Proceedings of the Institution of Civil Engineers: Transport. 165 (2012) 81-5.

[18] EN1992-2, Eurocode 2- Design of concrete structures, Part 2: Concrete bridges -Design and detailing rules European Commitiee for Standardization, Brussels 2005.

[19] EN1993-1-9, Design of steel structures, Part 1-9: Fatigue European Committee for standardization, Brussels, 2009.

[20] R. You, D. Li, C. Ngamkhanong, R. Janeliukstis, S. Kaewunruen. Fatigue Life Assessment Method for Prestressed concrete sleepers. Frontiers in Built Environment. 3 (2017) 1-13.

[21] CEB, CEB-fip model code 1990, Design of concrete structures, Thomas Telford House, London, United kindom, 1993.

[22] EN1992-2, Design of concrete structures, part 2: concrete bridges design and detailing rules, European Committee for standardization, Brussels, 2005.

[23] K.Y.M. Loo. Fatigue behaviour of CFRP-repaired corroded RC beams Ph.D. Sydney, Australia: The University of New South Wales; 2010.

[24] A. Parvez. Fatigue behaviour of steel-fibre-reinforced concrete beams and prestressed sleepers Ph.D. Australia: The University of New South Wales; 2015.

[25] S.K. Liu Ping. Investigation of the Dynamic Buckling of Spherical Shell Structures Due to Subsea Collisions. Applied Sciences-Basel. 8 (2018) 5.

[26] T.B. Liu Ping, KAEWUNRUEN S. Vibration-Induced Pressures on a Cylindrical Structure Surface in Compressible Fluid Applied Sciences. 9 (2019) 2.

[27] S.K. Ping Liu, Bai-jian Tang. Dynamic Pressure Analysis of Hemispherical Shell Vibrating in Unbounded Compressible Fluid. Applied Sciences-Basel. 10 (2018) 9.

[28] A. Parvez, S.J. Foster. Fatigue of steel-fibre-reinforced concrete prestressed railway sleepers. Eng Struct. 141 (2017) 241-50.

[29] C. Ngamkhanong, D. Li, S. Kaewunruen, Impact capacity reduction in railway prestressed concrete sleepers with vertical holes, IOP Conference Series: Materials Science and Engineering, IOP Publishing Ltd Prague, Czech Republic, 2017.

[30] S. Kaewunruen, A.M. Remennikov. Impact capacity of railway prestressed concrete sleepers. Engineering Failure Analysis. 16 (2009) 1520-32.
[31] A. Sarja, E. Vesikari. Durability design of concrete structures. CRC Press, Espoo,Finland, 2004.
[32] L. Tian, L. Xila. Durability Design of Concrete Structures. China Civil Engineering Journal. 27 (1994) 47-55.
[33] Z. Guofan, J. Weiliang, G. Jinxin. Sturctural Reliability Theory. China Architecture & Building Press, Beijing,China, 2000.
[34] AS3600, Design of concrete structures, Standards Australia, Australia, 2009.
[35] R. You, K. Goto, C. Ngamkhanong, and S. Kaewunruen, Nonlinear finite element analysis for structural capacity of railway prestressed concrete sleepers with rail seat abrasion, *Eng. Fail. Anal.* **95**, 2019, 47-65.
[36] D. Li and S. Kaewunruen, Effect of extreme climate on topology of railway prestressed concrete sleepers, *Climate*. **7**, 2019, 17.
[36] R. Janeliukstis and S. Kaewunruen, A novel separation technique of flexural loading-induced acoustic emission sources in railway prestressed concrete sleepers, *IEEE Access*. **7**, 2019, 51426-51440.
[37] C. Ngamkhanong, D. Li, A.M. Remennikov, S. Kaewunruen, Dynamic capacity reduction of railway prestressed concrete sleepers due to surface abrasions considering the effects of strain rate and prestressing losses, *Int J. Struct Stab. Dyn*. **19**, 2019, 1940001.
[38] S. Kaewunruen, D. Li, A.M. Remennikov, T. Ishida, Dynamic resistance and rational design of railway prestressed concrete sleepers, *Proceedings of the fib Symposium 2019: Concrete - Innovations in Materials, Design and Structures*, 2019, 1477-1484.
[39] S. Kaewunruen, J.M. Sussman, A. Matsumoto, Grand challenges in transportation and transit systems, *Front. in Built Env*. **2**, 2016, 55.